Technical Report

Characterization of Corrosion Film on 12Cr-6Ni-Fe and 12Cr-6Ni-2.5Mo-Fe Alloy Steel Using X-ray Photoelectron Spectroscopy

Katsuhiro NISHIHARA* Shohki HATANAKA
Hiroko HORIGOME Kyohei KANKI

Abstract

In 12Cr-6Ni-Fe and 12Cr-6Ni-2.5Mo-Fe alloy steel, corrosion resistance improves through change of the corrosion film by the addition of molybdenum (Mo). However, the effect of the Mo addition and its influence on the corrosion film structure have not been clarified completely. Therefore, the aim of the present research is to clarify the influence that Mo addition to a base material alloy has on the corrosion film structure. This report shows that the effect of Mo addition on the structure of a corrosion film was discussed through the depth direction distribution of photoelectron intensity based on XPS and HAX-PES spectra measured using soft X-ray (Al-Kα, 1 487 eV) and hard X-ray (synchrotron radiation, 8 000 eV).

1. Introduction

In recent years, as global energy demand has increased and shallow wells have become depleted, there has been a shift towards extracting oil and natural gas from deeper, higher-pressure wells (**Fig. 1**).[1] These wells are commonly referred to as a "sour environment" due to the presence of highly corrosive hydrogen sulfide (H_2S) and carbon dioxide (CO_2), which create a severely corrosive environment for steels. To withstand such corrosive environments, oil country tubular goods (OCTG) used for drilling and transporting oil and natural gas, as well as line pipes (L/P) used for their transportation, are typically made from highly corrosion-resistant and high-strength alloys. These alloys often contain large amounts of expensive elements such as Cr, Ni, and Mo. For example, duplex stainless steels are alloyed with approximately 20–30% Cr, 4–8% Ni, and 2–4% Mo, while Ni based alloys contain around 19–30% Cr, 25–60% Ni, and 2–14% Mo. Furthermore, economic efficiency is also required. This includes aspects like improved productivity and reduced development costs of oil and gas wells.[1–3]

Nippon Steel Corporation has successfully developed stainless steels suitable for use in environments containing carbon dioxide (CO_2), chloride ions (Cl^-), and hydrogen sulfide (H_2S). In the past, OCTG environments with carbon dioxide gas have typically utilized 13Cr martensitic stainless steel. However, the emergence of sulfide stress cracking (SSC) as an issue in environments with trace amounts of hydrogen sulfide has posed a challenge. To address this problem, Nippon Steel developed a super 13Cr steel that incorporates Mo into the base alloy to enhance SSC resistance.[4] Additionally, by reducing the carbon content and ensuring weldability, an economical version called super 13Cr steel (13CrS), specifically designed for line pipes, was also developed and deployed.[5, 6] During this development process, Mo was added to enhance the SSC resistance of the super 13Cr steel by maintaining the integrity of the film formed on its surface when exposed to corrosive environments. This film (natural oxide film, passive film, or corrosion film) contributes significantly to improving the SSC resistance. However, specific details regarding this mechanism were previously unknown.

In general, when stainless steel (Ni-Cr-Fe based alloy) comes into contact with a corrosive environment containing oxygen, it is believed that a chromium oxide film (CrOx film) forms on the surface of the steel through two different mechanisms of corrosion reaction. The first mechanism is the outward diffusion mechanism, where chromium ions released from the base alloy due to an anodic reaction diffuse outwards toward the corrosive environment, and the corrosion reaction takes place on the surface of the film. The second

* Dr. Eng., Senior Researcher, Materials Microstructure Characterization Research Dept., Materials Characterization Research Lab., Advanced Technology Research Laboratories
1-8 Fuso-Cho, Amagasaki City, Hyogo Pref. 660-0891

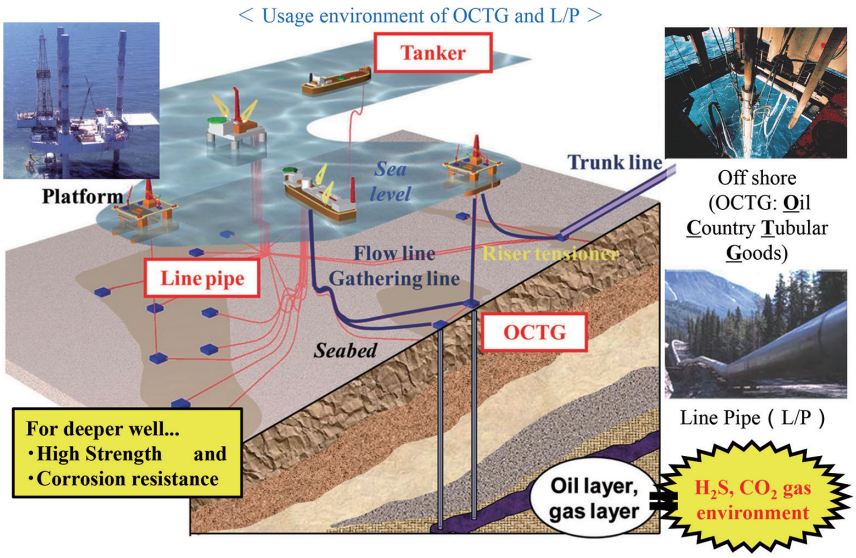

Fig. 1 Production and transportation in a severe oil and natural gas well environment[1)]

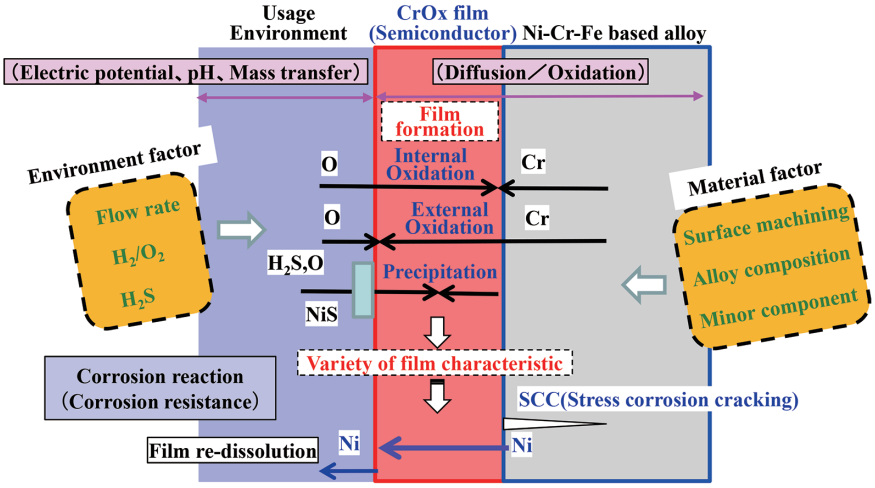

Fig. 2 Corrosion reaction on Ni-Cr-Fe based alloy steel in usage environment[7)]

mechanism is called the inward diffusion mechanism, where oxygen ions generated due to a cathodic reaction in the corrosive environment diffuse inward from the film surface towards the interface between the CrOx film and base alloy, leading to the corrosion reaction at this interface (**Fig. 2**).[7)] Therefore, by studying factors such as in-depth distributions and in-plane changes in terms of thickness, structure, crystallinity, elemental composition, and chemical bonding state of the CrOx film formed on the stainless steel, it becomes possible to estimate which corrosion reaction mechanism is taking place in that particular environment where the CrOx film has been formed.

The corrosion films formed on the surfaces of 12Cr-6Ni-Fe alloy steel and 12Cr-6Ni-2.5Mo-Fe alloy steel after the corrosion test were examined to a depth of about 30 nm for the elemental composition and chemical bonding state by photoelectron spectroscopy using soft X-rays (laboratory light source of Al-*Kα*/1 487 eV) and hard X-rays (synchrotron radiation of about 8 keV). We report the results of our investigation below.

2. Film Structure Analysis by Photoelectron Spectroscopy

We have been conducting research and development on evaluation and analysis techniques using photoelectron spectroscopy and other methods to nondestructively analyze structural changes in oxide films and corrosion films formed on steel surfaces. These techniques allow us to examine the elemental composition and chemical bonding state in both the depth direction and the in-plane direction of these films. In photoelectron spectroscopy, we irradiate a sample held in a vacuum with excitation light, which induces the emission of photoelectrons from the surface of the sample under the photoelectric effect. We then measure the intensity of these emitted photoelectrons as a function of their kinetic energy (photoelectron spectrum). By referencing the Fermi level, which represents the highest energy level occupied by electrons within the sample, we can convert this kinetic energy into binding energy. As a result, we obtain a photoelectron spectrum that reflects the binding energy dependence of emitted photoelectrons, providing information about the elemen-

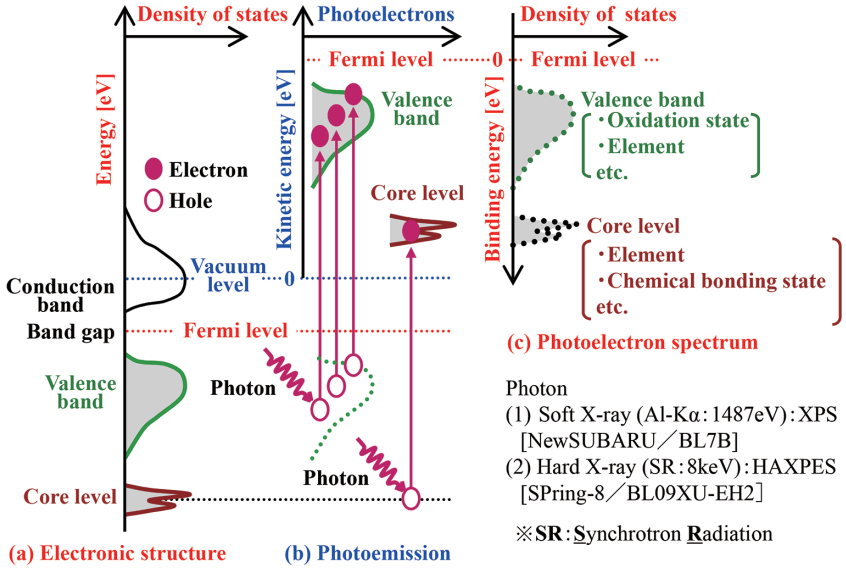

Fig. 3 X-ray photoelectron spectroscopy (XPS and HAXPES)[7)]

tal composition and chemical bonding state of the sample surface (**Fig. 3**).[7)]

The detection depth in photoelectron spectroscopy is influenced by the distance that electrons, excited by light irradiation within a solid, travel through the material without losing energy. This determines how far these electrons can reach the surface and can be emitted into the vacuum. In essence, the detection depth is governed by the mean free path of these electrons. When the kinetic energy of detected photoelectrons exceeds several tens of electron volts, the detection depth increases with the increase in kinetic energy. For instance, when using soft X-rays (Al-*Kα*/1 487 eV) as excitation light, the detection depth is a few nanometers. On the other hand, when utilizing hard X-rays (synchrotron radiation of about 8 keV), the detection depth extends to around 20 to 30 nm (**Fig. 4**).[7, 8)]

We conducted a nondestructive analysis to investigate the in-depth distribution of chemical bonding states within the surface layer of the film, about several nanometers deep from the film surface. This analysis utilized X-ray photoelectron spectroscopy (XPS) with soft X-rays from a laboratory light source, specifically Al-*Kα*/1 487 eV and Mg-*Kα*/1 254 eV.[9, 10)] Previous methods for analyzing in-depth changes in chemical bonding states, such as FIB milling combined with cross-sectional TEM observation or Ar^+ sputtering combined with surface analysis, were destructive and limited to examining changes from the film surface to near the buried film/steel interface. There were no effective nondestructive methods available for analyzing the chemical bonding states. To address this limitation, we attempted nondestructive analysis of the elemental composition and chemical bonding state distribution from the corrosion film's surface on the steel to the vicinity of the buried film/steel interface using hard X-ray photoelectron spectroscopy (HAXPES).[11–16)] HAXPES utilizes hard X-rays with a detection depth of about 20 to 30 nm, achieved through synchrotron radiation at around 8 keV.

3. Experimental Procedures

The chemical compositions of the test steels (12Cr-6Ni-Fe alloy steel and 12Cr-6Ni-2.5Mo-Fe alloy steel) are shown in **Table 1**. Each sample, with a thickness of 2 mm, was cut into a 10 mm square shape, and only one surface (measurement surface) was mirror polished. The 10 mm square samples were immersed in an etching solution simulating a sour oil or gas well environment for 2 and 24 hours. The etching solution had a pH of 4.0 and consisted of a 10% NaCl aqueous solution saturated with 10% H_2S+CO_2 gases.

First, we conducted the XPS spectrum measurement of the oxide/corrosion films formed on 12Cr-6Ni-Fe and 12Cr-6Ni-2.5Mo-Fe, using soft X-rays. The measurements were performed with a VG

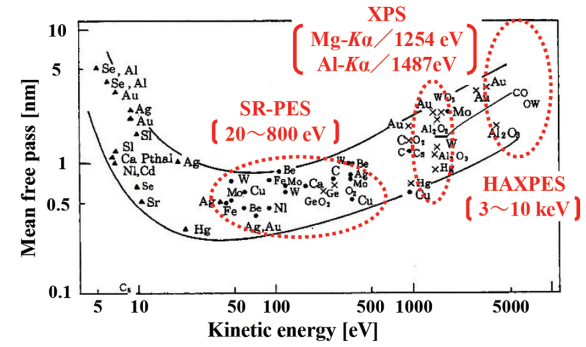

(a) Mean free pass of electron in material [8)]

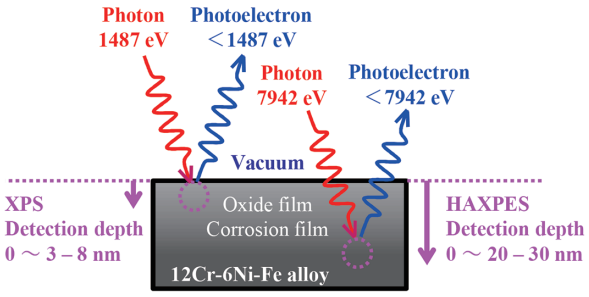

(b) Detection depth of XPS and HAXPES [7)]

Fig. 4 Detection depth of photoelectron spectroscopy (mean free pass of electron in material)[7, 8)]

Scienta R3000 XPS analyzer with ultra-high vacuum specifications, along with a laboratory light source of Al-$K\alpha$/1 487 eV. The experiment took place at the beam line BL7B in the NewSUBARU synchrotron radiation facility at the University of Hyogo Laboratory of Advanced Science and Technology for Industry. During the XPS spectrum measurement, soft X-rays were directed onto the sample's surface from an inclined angle of 45°. The emitted photoelectrons traveled in the same direction at a 45° angle and were detected within a vacuum. Additionally, the beam diameter of the soft X-rays irradiating the sample's surface was approximately 3 mm.

Subsequently, we conducted angle-resolved HAXPES (hard X-ray photoelectron spectroscopy) measurements. The experiment utilized a three-dimensional spatial resolution HAXPES unit located at the beam line BL09XU-EH2 of the SPring-8 synchrotron radiation facility. During the measurements, we obtained angle-resolved HAXPES spectra to capture the depth profile of elemental composition and chemical bonding states from the surface of the film to the interface between the buried film and base alloy.[14–16] To achieve this, hard X-rays with a synchrotron radiation energy of 7.94 keV were focused on a 11 μm (horizontal)×2 μm (vertical) beam and were directed onto the sample. The emitted photoelectrons within a detection angle range of 35°±32° relative to the sample surface were detected using a wide-angle objective lens, an electrostatic hemispherical electron energy analyzer, and a two-dimensional microchannel plate (MCP) detector. In traditional angle-resolved measurements, multiple measurements were required as the sample was rotated at various angles of incidence for X-ray irradiation or detection angles for the emitted photoelectrons from the sample. This method was time-consuming. However, in our angular dispersion measurement approach, a single measurement allowed us to obtain a two-dimensional distribution image of photoelectron emission intensity (with the vertical axis representing detection angles ranging from 23° to 87° divided into 225 divisions and the horizontal axis representing kinetic energy on an arbitrary scale). Consequently, nondestructive analysis of the film's elemental composition and chemical bonding state throughout its depth could be achieved in less than one-tenth of the time compared to the conventional angle-resolved measurements (see **Fig. 5**).[14–16]

Table 1 Chemical composition of lab melted test specimens

(mass%)

Mark	C	Ni	Cr	Mo	Fe
12Cr-6Ni-Fe	0.01	6.0	12.0	< 0.01	balanced
12Cr-6Ni-2.5Mo-Fe	0.01	6.0	12.0	2.5	balanced

4. Results

4.1 Structural analysis of steel surface film using soft X-ray photoelectron spectroscopy

Soft X-ray photoelectron spectroscopy (XPS) with a laboratory light source of Al-$K\alpha$/1 487 eV was utilized to analyze the chemical bond state changes with the progress of corrosion from the surface of the film formed on the steel surface to a depth of several nanometers. In general, when Ni-Cr-Fe based alloy steel, such as stainless steel, is exposed to an oxygen-containing environment, a composite oxide film predominantly composed of Cr oxide and Fe oxide is formed on its surface. To determine the composition ratio of the Cr oxide and Fe oxide in this composite oxide film, we examined the relative peak intensity ratio between the Cr $2p_{3/2}$ peak attributed to Cr oxide and the Fe $2p_{3/2}$ peak attributed to Fe oxide in our XPS spectra. The relative intensity ratio of Cr $2p_{3/2}$/(Cr $2p_{3/2}$+Fe $2p_{3/2}$) was calculated as an estimation of this composition ratio for the composite oxide film on the steel surface. Our results showed that this ratio of the steel with Mo added to base alloy was bigger than one of the base alloy and exhibited a greater proportion of CrOx within the corrosion film (**Figs. 6** and **7**).[10]

In Fig. 7, the relative peak intensity ratio of the natural oxide film before the corrosion test, when exposed to the atmosphere at normal temperature and pressure, was about 0.1. Subsequently, after 24 hours of immersion in the sour environment-simulating etching solution (with pH4.0, 10% NaCl aqueous solution, and 10% H_2S+CO_2 gas saturation), the relative peak intensity ratio of the natural oxide film increased to about 0.4. Interestingly, this change was independent of whether Mo was added or not. However, when the corrosion film was examined after 2 hours of immersion, distinct differences emerged. In the steel without Mo addition, the relative peak intensity ratio remained at approximately 0.1. In contrast, the steel with the Mo addition exhibited a significantly higher relative

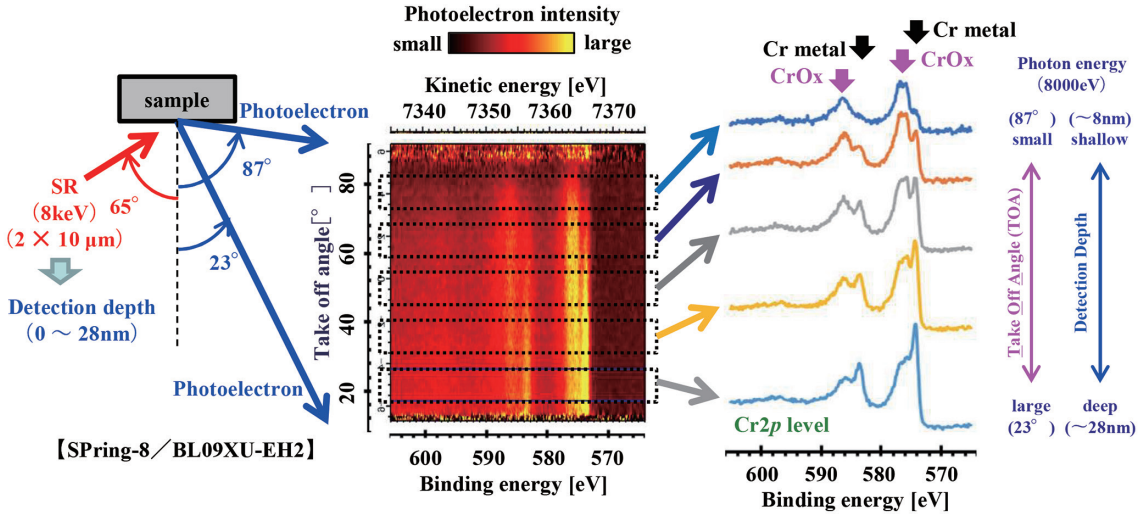

Fig. 5 Angle-resolved hard X-ray photoelectron spectroscopy[14–16]

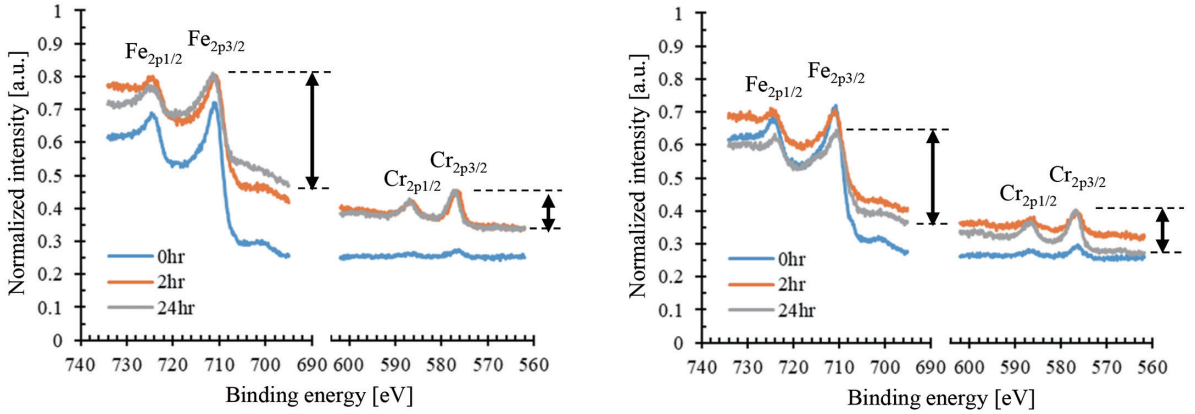

Fig. 6 Change in XPS spectra of 12Cr-6Ni-Fe and 12Cr-6Ni-2.5Mo-Fe with immersion time[10)]

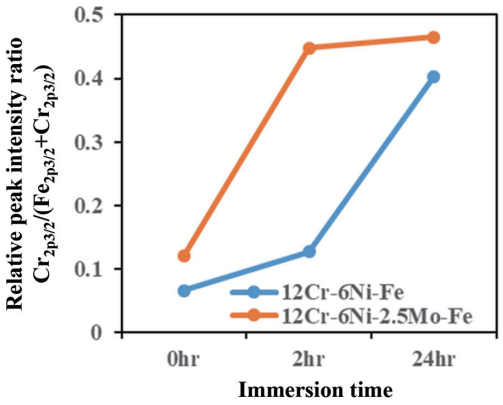

Fig. 7 Change in relative peak intensity ratio of 12Cr-6Ni-Fe and 12Cr-6Ni-2.5Mo-Fe with immersion time[10)]

peak intensity ratio, exceeding 0.4. This observation suggests that the addition of Mo to the base metal alloy accelerates the formation of CrOx on the alloy's surface during the early stage of corrosion when exposed to the sour environment-simulating etching solution. Consequently, this enhancement contributes to improved corrosion resistance.

4.2 Structural analysis of steel surface film using hard X-ray photoelectron spectroscopy

By angle-resolved HAXPES measurements of 12Cr-6Ni-Fe and 12Cr-6Ni-2.5Mo-Fe, the dependence of photoelectron emission intensity on the binding energy and detection angle (detection depth) was measured as a two-dimensional distribution image. Then, we extracted the photoelectron detection angle, that is, the HAXPES spectrum divided into five in the depth direction (**Fig. 8**).[16)]

First, focusing on the Fe $2p_{1/2}$ and Fe $2p_{3/2}$ peak shapes of 12Cr-6Ni-Fe, it was confirmed that Fe exists as FeOx oxide throughout the entire film from the surface of the corrosion film to the deep region near the base metal interface. Additionally, it was observed that as we went deeper into the film, peaks attributed to metallic Fe became more prominent. Similarly, based on the shapes of the Cr $2p_{1/2}$ and Cr $2p_{3/2}$ peaks originating from the base metal, it was confirmed that Cr exists as CrOx oxide throughout the corrosion film and that the peak intensity increased as we moved from the surface to the deeper region of the film. On the other hand, the peaks attributed to S and O originating from their presence in the corrosive environment (S 1*s* and O 1*s*) showed maximum intensity at the surface of the corrosion film and decreased in the deeper region of the corrosion film. From the shape of the S 1*s* peak, it was confirmed that most of S existed as sulfide with a small amount of sulfate SOx present. Furthermore, in the O 1*s* peak, two peak components were detected around 530 eV and 532 eV, with relative intensities increasing at about 530 eV near the surface and about 532 eV in the deeper region of the corrosion film. In the C 1*s* peak, two peak components attributed to contaminant C and carbonate CO_3^{2-} were detected. The intensities of these peaks were found to be minimal at or near the surface region while increasing in the deeper region of the corrosion film (Fig. 8 (a)).[16)]

Next, focusing on the Fe $2p_{1/2}$ and Fe $2p_{3/2}$ peaks arising from the base alloy of 12Cr-6Ni-2.5Mo-Fe, we found that FeOx oxide existed in a larger amount than the Fe metal only in the surface layer of the corrosion film. Inside the corrosion film, the intensity of the peak attributed to the metal Fe became relatively stronger than the peak attributed to the oxide FeOx in the deeper region. The peak intensity of the entire Fe 2*p* level also increased. Similarly, for the Cr $2p_{1/2}$ and Cr $2p_{3/2}$ peaks, the peak intensities were lowest in the surface layer and increased as the depth increased. From the peak shape, it was confirmed that the oxide CrOx was more dominant than the metal Cr in the surface layer of the film, but the proportion existing as the metal Cr increased in the film. On the other hand, the S 1*s*, O 1*s*, and C 1*s* peaks caused by the corrosive environment had the highest peak intensity at the surface layer of the corrosion film and decreased as the depth increased. From the S 1*s* and C 1*s* peaks, it was confirmed that S exists as sulfide and C exists as contaminant C throughout the corrosion film. In addition, the O 1*s* peak has two peak components near 530 eV and 532 eV, as in the case of the 12Cr-6Ni-Fe alloy. Still, throughout the corrosion film, the peak intensity near 530 eV was larger than the peak intensity near 532 eV, confirming that the oxide state is dominant (Fig. 8 (b)).[16)]

Furthermore, the Mo $3p_{1/2}$ and Mo $3p_{3/2}$ peaks originating from the base metal exhibited the lowest intensity at the surface layer, similar to Fe and Cr, and their intensities increased with depth. Analysis of the peak shapes confirmed that the sulfide MoSx and the oxide CrOx were more dominant than the metallic Mo in the surface layer of the film. However, in the deeper region, there was an increasing proportion of the metallic Mo present (**Fig. 9**).[16)]

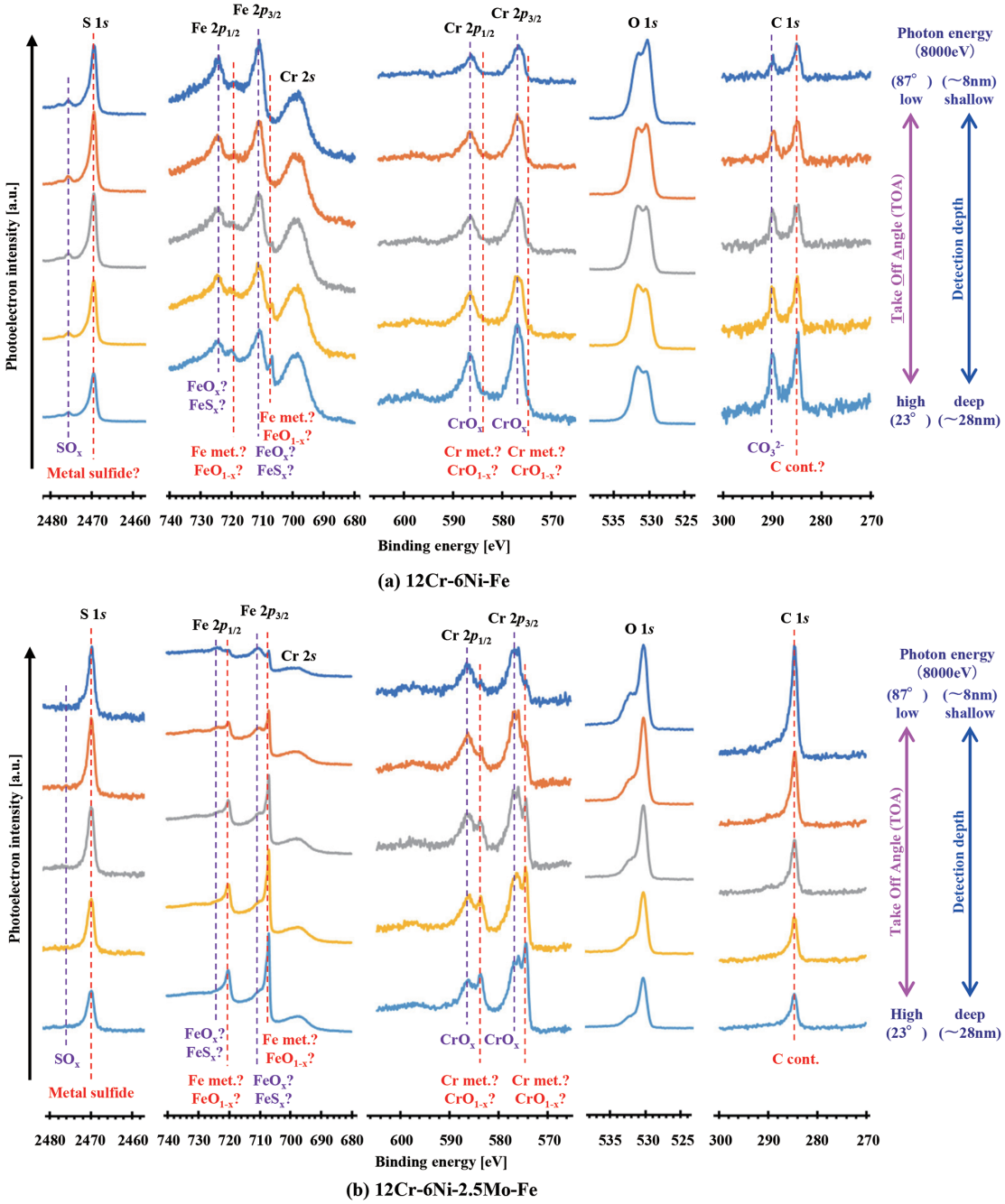

Fig. 8 Change in HAXPES spectra of 12Cr-6Ni-Fe and 12Cr-6Ni-2.5Mo-Fe with take off angle[16)]

Subsequently, the peak intensities of the core levels (Fe 2*p*, Cr 2*p*, Mo 3*p*) associated with the base alloy elements and the core levels (S 1*s*, C 1*s*, O 1*s*) associated with the elements in the corrosive environment were determined. Normalization was carried out to set the maximum value as 1.0, allowing for an analysis of the relative change in peak intensity along the depth direction. In this analysis, each core level's peak intensity was measured as the area intensity encompassing all chemical bonding states, including the metals and oxides (**Fig. 10**).[16)]

In 12Cr-6Ni-Fe, which is the basic composition of the base alloy, the peak intensities of Fe 2*p* and O 1*s* decreased continuously from the surface of the corrosion film to the deeper region. On the other hand, the peak intensities of Cr 2*p* and C 1*s* were lowest at the surface layer of the corrosion film and tended to increase as the depth increased. There was a region in the middle layer of the corrosion film where the tendency for the peak intensities to increase was small. In addition, the S 1*s* peak intensity tended to increase once and then decrease as the depth increased from the surface layer of the corrosion film. It was confirmed that there was a region in the middle layer of the corrosion film where the change in peak intensity was small (Fig. 10(a)).[16)] On the other hand, for 12Cr-6Ni-2.5Mo-Fe, both Fe 2*p* and Cr 2*p* peak intensities tended to increase as the depth from the surface of the corrosion film increased (Fig. 10(b)).[16)] In addition, in 12Cr-6Ni-Fe, the C 1*s* peak became larger

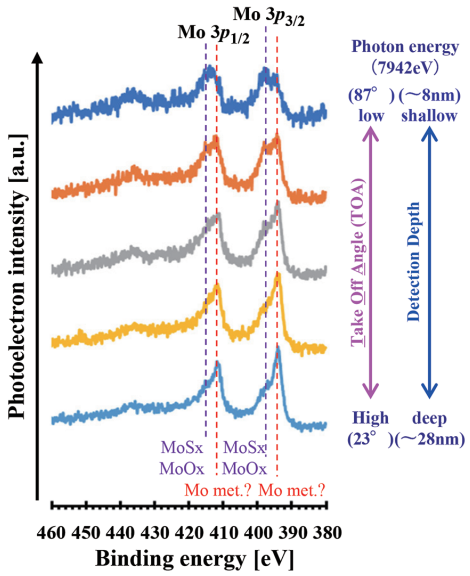

Fig. 9 Change in Mo 3*p* spectrum of 12Cr-6Ni-2.5Mo-Fe with take off angle[16)]

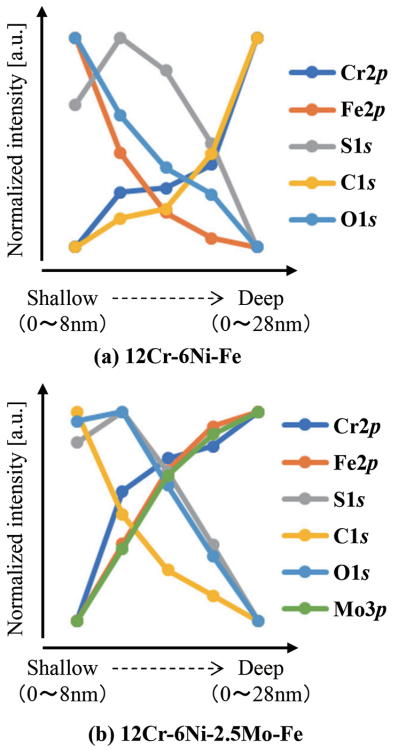

Fig. 10 Depth direction distribution of photoelectron intensity in HAXPES spectra of 12Cr-6Ni-Fe and 12Cr-6Ni-2.5Mo-Fe[16)]

as the depth increased from the surface layer of the corrosion film. Still, in 12Cr-6Ni-2.5Mo-Fe, the opposite tendency appeared, increasing closer to the surface layer of the corrosion film. When Mo is added to the base alloy, the formation of a corrosion film containing CO_3^{2-} as well as FeOx and CrOx is suppressed, and the peak components due to the metal Fe and metal Cr originating from the base alloy become prominent. The results suggest that the corrosion reaction of the base metal alloy is suppressed.

5. Conclusions

The elemental composition and chemical bonding states in the corrosion films formed on 12Cr-6Ni-Fe and 12Cr-6Ni-2.5Mo-Fe were measured by photoelectron spectroscopy (XPS) using soft X-rays (laboratory light source of Al-*Kα* 1487 eV) and by angle-resolved hard X-ray photoelectron spectroscopy (HAXPES) using hard X-rays (synchrotron radiation of about 8 keV). As a result, in the XPS spectrum (at a depth of several nanometers from the surface), it was confirmed that the relative intensity ratio Cr $2p_{3/2}$ / (Cr $2p_{3/2}$+Fe $2p_{3/2}$) of the Cr $2p_{3/2}$ peak attributed to CrOx to the Fe $2p_{3/2}$ peak attributed to FeOx increased with the progress of corrosion. It was also confirmed that the relative intensity ratio Cr $2p_{3/2}$/(Cr$2p_{3/2}$ +Fe $2p_{3/2}$) was higher when Mo was added to the base alloy than when Mo was not added. Also, the in-depth distribution of the chemical bonding state from the surface of the corrosion film to the vicinity of the base alloy interface to a depth of about 30 nm was revealed from the change in the HAXPES spectrum in the depth direction. Results were obtained that suggest the effect of the elemental composition of the base alloy on the in-depth distribution of inorganic compounds of Fe, Cr, Mo, etc. (CrOx, FeOx, FeS, MoOx, MoSx, etc.) in the corrosion film.

Acknowledgments

We would like to express our sincere gratitude to Associate Professor/Dr. Yuichi Haruyama of the University of Hyogo Laboratory of Advanced Science and Technology for Industry for his great cooperation and support in conducting joint research at the beam line BL7B of the University of Hyogo synchrotron radiation facility "New SUBARU".

We would also like to thank Professor/Dr. Kojiro Mimura and his students at the Osaka Metropolitan University and Dr. Akira Yasui of the Japan Synchrotron Radiation Research Institute (JASRI) for their great cooperation and support in the angle-resolved hard X-ray photoelectron spectroscopy measurements at the beam line BL09XU-EH2 of the synchrotron radiation facility SPring-8. This research would not have been possible without their assistance. We would like to take this opportunity to express our sincere gratitude to all of them.

References

1) Sagara, M. et al.: Nippon Steel & Sumitomo Metal Technical Report. (107), 59 (2015)
2) Takabe, H. et al.: Nippon Steel & Sumitomo Metal Technical Report. (107), 24 (2015)
3) Omura, T. et al.: Nippon Steel & Sumitomo Metal Technical Report. (107), 18 (2015)
4) Ueda, M. et al.: Corrosion/92. Paper No.55, NACE International, 1992
5) Ueda, M. et al.: Proceedings of Eurocorr/96. SessionVII, 1996
6) Miyata, Y. et al.: Kawasaki Steel Technical Report. (38), 53 (1998)
7) Nishihara, K.: Journal of Chemical Engineering of Japan. 86 (8), 391 (2022)
8) Brundle, C. R.: J. Vac. Sci. Technol. 11, 212 (1974)
9) Yamazui, H. et al.: Journal of Surface Science Society of Japan. 37 (4), 150 (2016)
10) Kanki, K. et al.: Corrosion, 79 (5), 570 (2023)
11) Doi, T. et al.: SPring-8/SACLA Research Report B. 5 (1), 97 (2017)
12) Cho-ying Lin et al.: SPring-8/SACLA Research Report A. 6 (2), 190 (2018)
13) Yoshiki, M. et al.: SPring-8/SACLA Research Report A. 8 (2), 432 (2020)
14) Takagi, K. et al.: SPring-8/SACLA Research Report A, 10 (4), 365 (2022)
15) Ikenaga, E. et al.: J. Electron Spectrosc. Relat. Phoenom. 190, 180 (2013)
16) Nishihara, K. et al.: https://support.spring8.or.jp/report/Report_JSR/PDF_JSR_2021B/2021B1737.pdf

Katsuhiro NISHIHARA
Dr. Eng., Senior Researcher
Materials Microstructure Characterization Research Dept., Materials Characterization Research Lab.
Advanced Technology Research Laboratories
1-8 Fuso-Cho, Amagasaki City, Hyogo Pref. 660-0891

Shohki HATANAKA
Amagasaki Technical Support Dept.
R & D Planning Div.

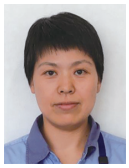

Hiroko HORIGOME
Amagasaki Technical Support Dept.
R & D Planning Div.

Kyohei KANKI
Researcher
Steel Products Research Dept.
Kansai R & D Lab.